Existence of spatial patterns in reaction–diffusion systems incorporating a prey refuge[*]

Lakshmi Narayan Guin, Santabrata Chakravarty[1], Prashanta Kumar Mandal

Department of Mathematics, Visva-Bharati
Santiniketan-731 235, West Bengal, India
guin_ln@yahoo.com; santabrata2004@yahoo.co.in;
prashantakumar.mandal@visva-bharati.ac.in

Abstract. In real-world ecosystem, studies on the mechanisms of spatiotemporal pattern formation in a system of interacting populations deserve special attention for its own importance in contemporary theoretical ecology. The present investigation deals with the spatial dynamical system of a two-dimensional continuous diffusive predator–prey model involving the influence of intra-species competition among predators with the incorporation of a constant proportion of prey refuge. The linear stability analysis has been carried out and the appropriate condition of Turing instability around the unique positive interior equilibrium point of the present model system has been determined. Furthermore, the existence of the various spatial patterns through diffusion-driven instability and the Turing space in the spatial domain have been explored thoroughly. The results of numerical simulations reveal the dynamics of population density variation in the formation of isolated groups, following spotted or stripe-like patterns or coexistence of both the patterns. The results of the present investigation also point out that the prey refuge does have significant influence on the pattern formation of the interacting populations of the model under consideration.

Keywords: predator–prey, prey refuge, Turing pattern, diffusion-driven instability.

1 Introduction

In recent times, major attention has been focused on the studies concerning the spatiotemporal pattern formation in reaction-diffusion systems in modern mathmatical biology and ecology because of the most exciting and challenging problems in this domain. In 1952, Alan Turing first showed mathematically in his seminal paper [47] that a system of coupled nonlinear reaction-diffusion equations could give rise to spatial concentration patterns of a fixed characteristic length from an arbitrary initial configuration due to diffusion-driven instability. The model for spatially extended system generally involves

---

[1]Corresponding author.

the interaction between the predator and the prey, that is, the reaction item and the diffusion item comes into being the predator's "pursuit" and the prey's "evasion" [3, 27, 30, 39, 40]. Usually, diffusion is considered as a spatial transmission way, which moves from high concentration to low concentration. Turing suggested that in a reaction-diffusion system describing the interaction between two species, different diffusion rates can lead to the destabilization of a constant steady state, followed by the transition to a nonhomogeneous steady state. According to this result, a steady state is Turing unstable if it is stable as a solution to the reaction system without diffusion terms, but unstable as a solution of the full reaction-diffusion system. This mechanism, known as diffusion-driven instability, leads to the formation of spatial patterns [6, 12, 34, 41, 42, 45]. This remarkable idea has been playing significant role in theoretical ecology, embryology and other branches of science [31, 32]. In 1972, Segel and Jackson [37] called attention to the Turing's ideas that would be also applicable in population dynamics. During this period of time, Gierer and Meinhardt [8] provided with a biologically justified formulation of a Turing model and studied its properties through numerical simulations. Levin and Segel [23] suggested that the scenario of spatial pattern formation is a possible origin of planktonic patchiness. Haque [15] investigated the emergence of complex patterns in the Beddington–DeAngelis predator–prey model and their simulations reveal that the typical dynamics of population density variation is the formation of isolated groups. In recent years there has been considerable interest in spatial and temporal behavior of interacting species in ecosystems. The dynamical behaviour between predator and prey has long been and will continue to be one of the dominant themes in ecosystems due to its universal existence and importance [1, 11, 20, 25, 48, 50].

Prey may avoid being killed by predators either by defending themselves or by escaping. One way to escape is to move into a refuge where predation risk is reduced [29, 33]. Recently, several scholars have pointed out that in many situations, there was a constant proportion of prey which were protected from predation by refuge. Some theoretical studies through suitable mathematical models and a number of experiments indicated that refugia had a stabilizing effect on the dynamics of predator–prey interactions and prey extinction can be prevented by the addition of refuges [9, 17, 27, 35, 38, 46, 49].

Connell [7] recognized an example from nature in which the spatial refuge of the barnacle Balanus glandula in the higher intertidal may contribute to the stability of its interaction with the predatory snails Thais. Larvae of western flower thrips *Frankliniella occidentalis* use the web produced by spider mites as a refuge from predation by the predatory mite *Neoseiulus cucumeris*. Magalhaes et al. [26] tested how the presence of a refuge affects the population dynamics of western flower thrips (*Frankliniella occidentalis Pergande*) and its predator, the phytoseiid mite *Neoseiulus* (*Amblyseius*) *cucumeris* (*Oudemans*) which is a major pest of greenhouse crops. In this way, some fraction of the prey population is partially protected against predators [10]. Hassel [16] showed that adding a large refuge to a model, which exhibited divergent oscillations in the absence of refuge, replaced the oscillatory behaviour with a stable equilibrium. Chen et al. [5] concluded that the prey refuge has no influence on the persistence property of both predator and prey species and the prey refuge could influence the densities of both prey and predator species greatly. Ko and Ryu [21] investigated the asymptotic behaviour of spatially

inhomogeneous solutions and the local existence of periodic solutions of a predator–prey model incorporating prey refuge under the zero-flux Neumann boundary conditions.

The effect of the use of refuges by the prey population on the temporal dynamics of a predator–prey model has been investigated by many eminent researchers [5, 18, 21, 22, 28, 36]. However, to the best of our knowledge, little attention has been paid to the dynamics of a spatiotemporal predator–prey model incorporating prey refuges. Now, it is usual to inquire how the prey refuge has an effect on the spatiotemporal dynamics of a reaction–diffusion predator–prey model. Assuming the importance of constant proportion of prey refuges and Turing spatial pattern formation on predator–prey model in ecology, an attempt has been made here to investigate the influence of prey refuges and diffusion in a prey-dependent predator–prey model which is an updation of the following model studied extensively by Bazykin et al. [4]:

$$\frac{\mathrm{d}u}{\mathrm{d}t} = ru\left(1 - \frac{u}{k}\right) - \frac{auv}{u + c}, \tag{1a}$$

$$\frac{\mathrm{d}v}{\mathrm{d}t} = -\mathrm{d}v + \frac{buv}{u + c} - hv^2, \tag{1b}$$

$$u(0) > 0, \quad v(0) > 0, \tag{1c}$$

where u, v denote prey and predator population size respectively at any instant t, and biologically meaningful constants viz. r, k, a, b, c, d, h are all positive. Here r designates the intrinsic growth rate and k, the carrying capacity of the prey species; a is the predation rate or capturing rate of prey by predator; b is the maximal predator growth rate; c is the interference coefficient of the predator; d is the predator natural mortality rate; h is the predator intra-species competition. Competition among members of the same species, known as intra-species competition is often observed in ecology. It refers to a decrease in reproduction or an increase in death rate with an increase in predator density. Models with intra-species competition have been extensively studied in literature [4,13,15]. However, the effect of prey refuges on the spatiotemporal dynamics of a reaction–diffusion predator–prey system has not been reported there. As a result, the main aim of this investigation is to study the influences of prey refuge on the spatiotemporal dynamics of a reaction–diffusion system with prey-dependent Holling type II functional response. This work is an attempt to make a bridge between the effect of prey refuge on the temporal dynamics of a predator–prey model and the influence of prey refuges on the spatiotemporal dynamics of a reaction–diffusion predator–prey system through numerical simulations.

The present article is organized as follows. Basic preliminaries of a spatial predator–prey model are included in Section 2. In this section, the existence of all possible positive equilibria and their dependence on the refuge parameter has been investigated. In Section 3, the stability of the proposed model without diffusion has been analyzed. The stability of the diffusive model alongwith the mathematical expression for Turing space has been discussed in Section 4. Section 5 illustrates the emergence of Turing patterns through numerical simulations. Finally, some conclusions and comments based on numerical simulations exhibiting quantitative response of the system are included in Section 6.

2 The model and analysis

The above model (1) has been wisely updated in the present study by incorporating constant proportion of refuge protecting mu of the prey, where $m \in [0,1)$ is constant. This leaves $(1-m)u$ of the prey available to the predator and hence model (1) has been modified to the following form:

$$\frac{\mathrm{d}u}{\mathrm{d}t} = ru\left(1 - \frac{u}{k}\right) - \frac{a(1-m)uv}{(1-m)u+c} = f_1(u,v), \tag{2a}$$

$$\frac{\mathrm{d}v}{\mathrm{d}t} = -\mathrm{d}v + \frac{b(1-m)uv}{(1-m)u+c} - hv^2 = f_2(u,v), \tag{2b}$$

$$u(0) > 0, \quad v(0) > 0. \tag{2c}$$

In the light of spatial pattern formation of above Bazykin's [4] model incorporating a prey refuge, a major step towards development has been performed with the following reaction–diffusion model:

$$\frac{\partial u}{\partial t} = f_1(u,v) + D_1\nabla^2 u, \tag{3a}$$

$$\frac{\partial v}{\partial t} = f_2(u,v) + D_2\nabla^2 v, \tag{3b}$$

$$u(0,x,y) > 0, \quad v(0,x,y) > 0, \tag{3c}$$

where $\nabla^2 \equiv \partial^2/\partial x^2 + \partial^2/\partial y^2$ the usual Laplacian operator in 2D space; D_1, D_2 are the diffusion coefficients for prey and predator, respectively. Assumming that the system parameters do not depend on space or time, that is, the environment is uniform.

In order to minimize the number of parameters involved in the proposed model (3), it is extremely useful to write the model in nondimensionalized form. By using the following change of variables: $\tilde{u} = u/k$, $\tilde{v} = va/(kb)$, $\tilde{t} = tr$, $\tilde{x} = x/L$, $\tilde{y} = y/L$ and the dimensionless parameters $\alpha = c/k$, $\epsilon = b/r$, $\gamma = d/r$, $\delta = hkb/(ar)$, $d_1 = D_1/(rL^2)$, and $d_2 = D_2/(rL^2)$; L being the characteristic length, one can obtain the nondimensional form of the system (3) as (after dropping tildes)

$$\frac{\partial u}{\partial t} = F_1(u,v) + d_1\nabla^2 u, \tag{4a}$$

$$\frac{\partial v}{\partial t} = F_2(u,v) + d_2\nabla^2 v, \tag{4b}$$

$$u(0,x,y) > 0, \quad v(0,x,y) > 0, \tag{4c}$$

where $F_1(u,v) = u(1-u) - \epsilon(1-m)uv/((1-m)u+\alpha)$ and $F_2(u,v) = -\gamma v + \epsilon(1-m)uv/((1-m)u+\alpha) - \delta v^2$.

Model (4) is to be analyzed under the following zero-flux boundary conditions:

$$\frac{\partial u}{\partial \nu} = \frac{\partial v}{\partial \nu} = 0, \quad (x,y) \in \partial\Omega,$$

where $\partial\Omega$ is the closed boundary of the reaction–diffusion domain Ω and ν is the unit outward normal vector of the boundary $\partial\Omega$, assuming to be smooth. $\partial u/\partial\nu$ and $\partial v/\partial\nu$ are respectively the normal partial derivatives of u and v on $\partial\Omega$. The main reason for choosing zero-flux boundary conditions is that we are interested in the self-organisation of pattern; zero-flux conditions imply no external input from outside.

The non-spatial model, i.e., without the diffusion terms of (4) has at most three ecologically meaningful equilibria (stationary states), which correspond to spatially homogeneous equilibria of the full spatial model (4) in $\mathbb{R}_+^2 = [(u, v): u \geqslant 0, v \geqslant 0]$ viz., (i) $e_0(0,0)$ (total extinction), (ii) $e_1(1,0)$ (extinction of the predator) and (iii) $e_2(u_2, v_2)$ (coexistence of predator and prey), where $v_2 = (1 - u_2)[(1 - m)u_2 + \alpha]/((1 - m)\epsilon)$; $u_2 \in (0, 1)$ and u_2 be the roots of the following cubic equation:

$$a_0 x^3 + 3a_1 x^2 + 3a_2 x + a_3 = 0 \quad (a_0 \neq 0) \tag{5}$$

with coefficients

$$\begin{aligned}
a_0 &= (1 - m)^2\delta, \\
3a_1 &= \delta(1 - m)\big[2\alpha - (1 - m)\big], \\
3a_2 &= (1 - m)^2\big[\epsilon(\epsilon - \gamma) - \delta\big] + \delta\big[\alpha - (1 - m)\big]^2, \\
a_3 &= -\big[(1 - m)\gamma\alpha\epsilon + \delta\alpha^2\big].
\end{aligned}$$

Equation (5) is now reduced to

$$z^3 + 3Hz + G = 0$$

by the transformation $z = a_0 x + a_1$. Equation (5) has exactly one real positive root if $G^2 + 4H^3 > 0$, where $G = a_0^2 a_3 - 3a_0 a_1 a_2 + 2a_1^3$, $H = a_0 a_2 - a_1^2$, and using Cardan's method, we obtain that the root is $(r_1 - H/r_1 - a_1)/a_0$, where r_1 denotes one of the three values of $[(-G + \sqrt{G^2 + 4H^3})/2]^{1/3}$. Considering the existence and feasibility of the interior equilibrium point $e_2(u_2, v_2)$ of non-spatial model of (4), throughout this article, we assume that $\alpha > (1 - m)/2$ and $\epsilon(\epsilon - \gamma) > \delta$.

3 Linear stability analysis for non-diffusive system

The non-spatial model, i.e., in the absence of diffusion terms of (4) can be written in the form $\dot{X} = F(X, \epsilon) = (F_1(u, v), F_2(u, v))^{\mathrm{T}}$ where $X = (u, v)^{\mathrm{T}}$. Here X^{T} represents the transpose of the matrix X. Now the Jacobian matrix

$$DF(X, \epsilon) = J = (\nabla F_1, \nabla F_2)^{\mathrm{T}} = \begin{bmatrix} \frac{\partial F_1}{\partial u} & \frac{\partial F_2}{\partial u} \\ \frac{\partial F_1}{\partial v} & \frac{\partial F_2}{\partial v} \end{bmatrix} \in \mathbb{R}^{2 \times 2},$$

of the non-spatial model of (4) at any arbitrary point (u, v) is given by

$$J = \begin{bmatrix} 1 - 2u - \frac{\epsilon(1-m)v\alpha}{[(1-m)u+\alpha]^2} & \frac{-\epsilon(1-m)u}{(1-m)u+\alpha} \\ \frac{\epsilon(1-m)v\alpha}{[(1-m)u+\alpha]^2} & -\gamma - 2\delta v + \frac{\epsilon(1-m)u}{(1-m)u+\alpha} \end{bmatrix} = (\Gamma_{ij})_{2 \times 2}.$$

We denote $J_k = J$, the Jacobian evaluated at e_k, $i = 1, 2$; $j = 1, 2$; $k = 0, 1, 2$ and the determinant $J_k = \det J_k$, trace $J_k = \operatorname{tr}(J_k)$.

3.1 The dynamical behaviours of the system around the boundary equilibrium points $e_0(0, 0)$ and $e_1(1, 0)$

Lemma 1.

   (i) *The equilibrium point $e_0(0, 0)$ always exists and it is a saddle point.*

   (ii) *The equilibrium point $e_0(1, 0)$ corresponding to extinction of the predator is a saddle point when $(1 - m)\epsilon > \gamma[(1 - m) + \alpha]$ or is locally asymptotically stable in the uv-plane when $(1 - m)\epsilon < \gamma[(1 - m) + \alpha]$.*

The proof of Lemma 1 is omitted here for the sake of brevity, interested readers are referred to [19].

3.2 The dynamical behaviour of the system around the interior equilibrium point $e_2(u_2, v_2)$

Lemma 2.

   (i) *The equilibrium point $e_2(u_2, v_2)$ is locally asymptotically stable iff*

$$\big[(1 - m)u_2 + \alpha\big]^2 < \Lambda_1 \quad and \quad \Lambda_2 > 0,$$

   where

$$\begin{aligned}
\Lambda_1 = {}& 4\alpha u_2{}^2 - \epsilon v_2 m\alpha + \epsilon u_2 m\alpha + 2\delta v_2 u_2{}^2 m^2 + 4\delta v_2 u_2 \alpha \\
& - 4\delta v_2 u_2{}^2 m - 4\delta v_2 u_2 m\alpha - 4u_2{}^3 m + 2u_2{}^3 m^2 + 2u_2 \alpha^2 \\
& + \gamma u_2{}^2 + \gamma \alpha^2 + 2u_2{}^3 - \epsilon u_2{}^2 - 2\gamma u_2 m\alpha - 2\gamma u_2{}^2 m \\
& + 2\gamma u_2 \alpha + \gamma u_2{}^2 m^2 - 4u_2{}^2 m\alpha + \epsilon v_2 \alpha + 2\epsilon u_2{}^2 m - \epsilon u_2{}^2 m^2 \\
& - \epsilon u_2 \alpha + 2\delta v_2 u_2{}^2 + 2\delta v_2 \alpha^2,
\end{aligned}$$

$$\begin{aligned}
\Lambda_2 = {}& -8u_2{}^3 \delta v_2 m - \epsilon u_2 m\alpha + 8u_2{}^2 \delta v_2 \alpha + 4u_2{}^3 \epsilon m + 4u_2{}^3 \delta v_2 \\
& - 2u_2{}^3 m^2 \epsilon - 2u_2{}^2 \alpha\epsilon - 2\delta v_2 u_2{}^2 m^2 - 4\delta v_2 u_2 \alpha + 4\delta v_2 u_2{}^2 m \\
& + 2u_2{}^2 \alpha\epsilon m + 4u_2{}^3 m^2 \delta v_2 + 4u_2 \alpha^2 \delta v_2 + 4\delta v_2 u_2 m\alpha - \gamma u_2{}^2 \\
& - \gamma \alpha^2 + \epsilon u_2{}^2 + 2\gamma u_2 m\alpha + 2\gamma u_2{}^2 m - 2\gamma u_2 \alpha - \gamma u_2{}^2 m^2 \\
& - 2\epsilon u_2{}^2 m + \epsilon u_2{}^2 m^2 + \epsilon u_2 \alpha - 2\delta v_2 u_2{}^2 - 2\delta v_2 \alpha^2 - 2\alpha\epsilon v_2{}^2 m\delta \\
& + 2\alpha\epsilon v_2{}^2 \delta - 4u_2{}^2 m\gamma\alpha + \alpha\epsilon v_2 \gamma - 2u_2{}^3 \epsilon - 8u_2{}^2 m\delta v_2 \alpha - 4u_2{}^3 \gamma m \\
& + 4u_2{}^2 \gamma\alpha + 2u_2{}^3 m^2 \gamma + 2u_2 \alpha^2 \gamma - \alpha\epsilon v_2 m\gamma + 2u_2{}^3 \gamma.
\end{aligned}$$

   (ii) *If $\gamma < \epsilon \leqslant 2\epsilon\delta/(1 - m)$ and $\underline{v} > 0$, then local stability of $e_2(u_2, v_2)$ ensures its global stability, where $\underline{v} = ((\epsilon - \gamma)(1 - m)\underline{u} - \alpha\gamma)/\delta((1 - m)\underline{u} + \alpha)$, $\underline{u} = (1 \pm \sqrt{1 - 4\epsilon\underline{v}})/2$.*
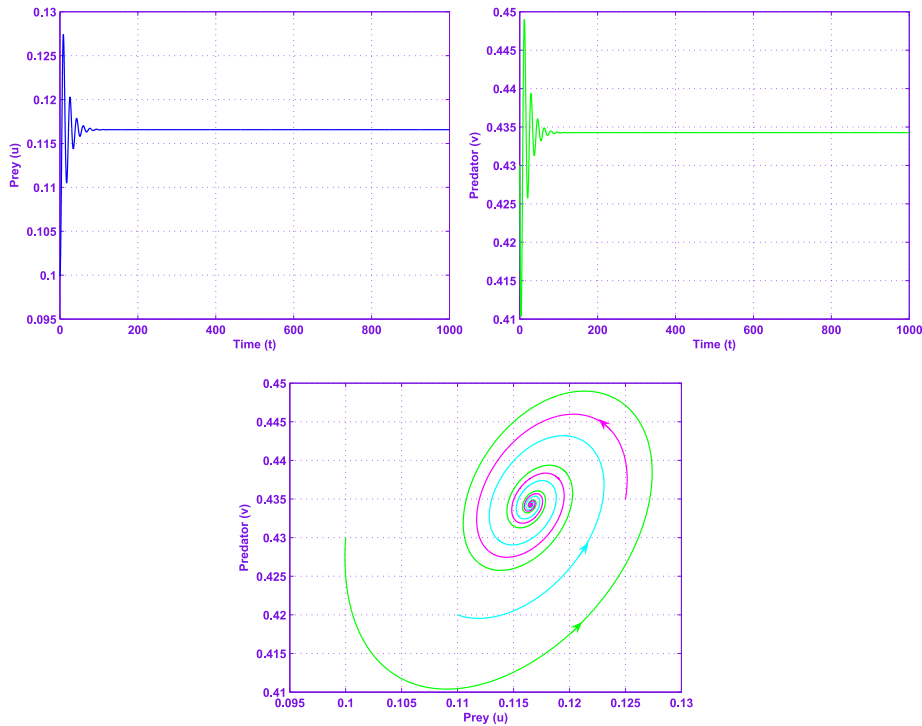
Fig. 1. Global stability of the non-spatial model of (4) around the positive interior equilibrium point e_2.

(iii) *The system admits a Hopf-bifurcation around $e_2(u_2, v_2)$ at $\alpha = \alpha^{[HB]}$, where $\alpha^{[HB]}$ is given by*

$$\alpha^{[HB]} = \frac{1}{2} \frac{(-2u_2 + 4u_2^2 + 4\delta v_2 u_2 - \epsilon u_2 + \epsilon v_2 + 2\gamma u_2 - \sqrt{\sigma})(-1 + m)}{\gamma + 2\delta v_2 - 1 + 2u_2},$$

$$\sigma = \epsilon^2 u_2^2 + \epsilon^2 v_2^2 + 8u_2^2 \epsilon v_2 - 2\epsilon^2 u_2 v_2 - 4u_2 \epsilon v_2 + 8\delta v_2^2 u_2 \epsilon + 4\epsilon v_2 \gamma u_2.$$

Proof. (i) Two eigenvalues of the Jacobian matrix J_2 at $e_2(u_2, v_2)$ are given by

$$\frac{1}{2}(\Gamma_{11} + \Gamma_{22}) \pm \sqrt{(\Gamma_{11} + \Gamma_{22})^2 - 4(\Gamma_{11}\Gamma_{22} - \Gamma_{12}\Gamma_{21})}$$

Therefore, by Routh–Hurwitz criteria, the proposed non-spatial model of (4) is locally asymptotically stable in the $uv-$plane around the interior equilibrium point $e_2(u_2, v_2)$ provided $\mathrm{tr}(J_2) = \Gamma_{11} + \Gamma_{22} < 0$ and $\det J_2 = \Gamma_{11}\Gamma_{22} - \Gamma_{12}\Gamma_{21} > 0$. Figure 1 depicts the global stability of the non-spatial model of (4) around the positive interior equilibrium point $e_2(0.1165668239, 0.4342664405)$ for $\alpha = 0.3$, $m = 0.2$, $\gamma = 0.02$, $\delta = 0.5$ and $\epsilon = 1.0$.
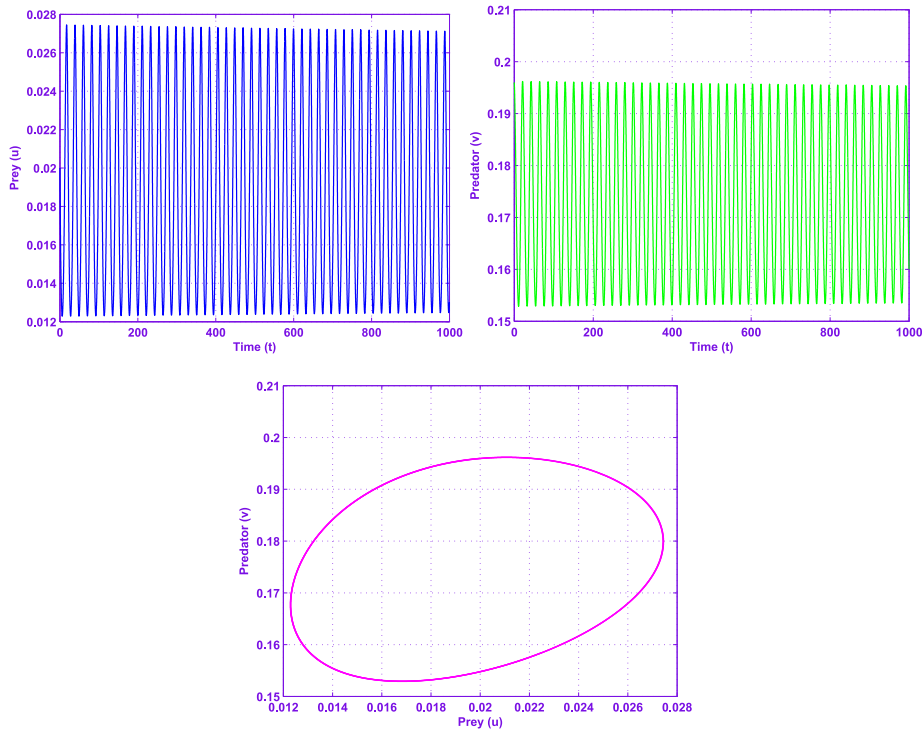
(ii) See Appendix.

Fig. 2. Hopf-bifurcation of the non-spatial model of (4) around the positive interior equilibrium point e_2 at $\alpha = \alpha^{[\text{HB}]}$.

(iii) At the equilibrium point $e_2(u_2, v_2)$, the characteristic equation is given by

$$\mu^2 - \text{tr}(J_2)\mu + \det J_2 = 0,$$

where $u - u_2 \approx \text{e}^{\mu t}$, $v - v_2 \approx \text{e}^{\mu t}$. If $\text{tr}(J_2) = 0$ at $\alpha = \alpha^{[\text{HB}]}$, then both the eigenvalues will be purely imaginary if $\det J_2 > 0$. Replacing $\mu = \mu_1 + \text{i}\mu_2$ into the corresponding characteristic equation and separating real and imaginary parts, we get

$$\left(\mu_1^2 - \mu_2^2\right) - \text{tr}(J_2)\mu_1 + \det J_2 = 0, \tag{6a}$$

$$2\mu_1\mu_2 - \text{tr}(J_2)\mu_2 = 0. \tag{6b}$$

Elementary differentiation of (6a) with respect to α and considering $\mu_1 = 0$, we get

$$\frac{\text{d}\mu_1}{\text{d}\alpha}\bigg|_{\alpha = \alpha^{[\text{HB}]}} = \frac{-\epsilon(1-m)(u_2 + v_2)}{[(1-m)u_2 + \alpha]^2} + \frac{2\alpha\epsilon(1-m)v_2}{[(1-m)u_2 + \alpha]^3} \neq 0.$$

Hence, the system goes through a Hopf-bifurcation at $\alpha = \alpha^{[\text{HB}]}$ around e_2. Figure 2 depicts the situation for Hopf-bifurcation of the non-spatial model of (4) around e_2 corresponding to the parameter values $m = 0.2$, $\gamma = 0.02$, $\delta = 0.5$, $\epsilon = 1.0$ and $\alpha = \alpha^{[\text{HB}]} = 0.126$. $\qquad\square$

4   Turing instability analysis

In this section, we deal with the analysis of Turing instability of the spatially positive steady state $e_2(u_2, v_2)$ of the present model system (4). To linearize the system (4) around $e_2(u_2, v_2)$ for small space and time-dependent perturbations, we assume

$$u(\overrightarrow{q}, t) = u_2 + \overline{u}(\overrightarrow{q}, t), \quad \left|\overline{u}(\overrightarrow{q}, t)\right| \ll u_2,$$
$$v(\overrightarrow{q}, t) = v_2 + \overline{v}(\overrightarrow{q}, t), \quad \left|\overline{v}(\overrightarrow{q}, t)\right| \ll v_2,$$

and

$$\begin{bmatrix} \overline{u}(\overrightarrow{q}, t) \\ \overline{v}(\overrightarrow{q}, t) \end{bmatrix} = \begin{bmatrix} \alpha_1 \\ \alpha_2 \end{bmatrix} e^{\mu t} e^{i \overrightarrow{k} \overrightarrow{q}}, \quad \overrightarrow{k} = (k_x, k_y),$$

where $\overrightarrow{q} = (x, y)$ designates the spatial vector in two dimensions; μ is the fluctuated growth rate in time t; α_1, α_2 are the corresponding amplitudes; $k\,(=|\overrightarrow{k}| = (k_x^2 + k_y^2)^{1/2})$ is the wave-number of the solution, and i represents imaginary number. The corresponding characteristic equation of the system (4) is

$$\left| J_2 - k^2 d - \mu I_2 \right| = 0, \tag{7}$$

$$J_2 = \begin{bmatrix} \Gamma_{11} & \Gamma_{12} \\ \Gamma_{21} & \Gamma_{22} \end{bmatrix}, \quad d = \begin{bmatrix} d_1 & 0 \\ 0 & d_2 \end{bmatrix}, \quad I_2 = \begin{bmatrix} 1 & 0 \\ 0 & 1 \end{bmatrix}.$$

The roots of (7) can be obtained by the following form:

$$\mu_{\pm}(k) = \frac{-B \pm \sqrt{B^2 - 4C}}{2}, \tag{8}$$

where

$$B(k^2) = k^2(d_1 + d_2) - \operatorname{tr} J_2, \tag{9}$$
$$C(k^2) = \det J_2 + k^4 d_1 d_2 - k^2(d_1 \Gamma_{22} + d_2 \Gamma_{11}). \tag{10}$$

System (4) will be unstable if at least one of the roots of (7) is positive. So, diffusion-driven instability can only be attained if $C(k^2) < 0$ and this condition guarantees that the coefficient of k^2 in (10) is positive, i.e.,

$$d_1 \Gamma_{22} + d_2 \Gamma_{11} > 0. \tag{11}$$

We find in equation (10) that $C(k^2)$ is a quadratic polynomial in k^2 and its extremum is minimum at

$$k_{\min}^2 = \frac{d_1 \Gamma_{22} + d_2 \Gamma_{11}}{2 d_1 d_2} > 0. \tag{12}$$

At $k^2 = k_{\min}^2$, $C(k^2) < 0$ transforms into

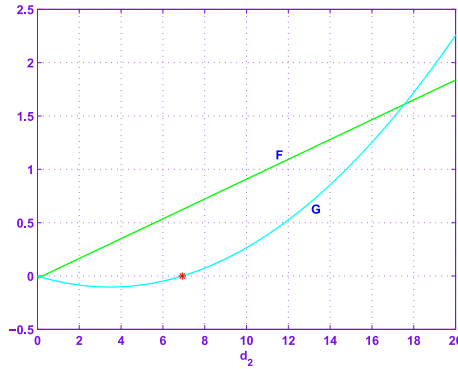$$(d_1 \Gamma_{22} + d_2 \Gamma_{11})^2 > 4 d_1 d_2 (\det J_2). \tag{13}$$

Fig. 3. Emergence of the Turing instability corresponding to $F = (d_1\Gamma_{22} + d_2\Gamma_{11})$ and $G = [(d_1\Gamma_{22} + d_2\Gamma_{11})^2 - 4d_1d_2(\det J_2)]$.

We summarize the necessary and sufficient conditions for the emergence of "Turing space" through diffusion-driven instability as follows:

  (i) $\mathrm{tr}(J_2) = (\Gamma_{11} + \Gamma_{22}) < 0$,   i.e., $[(1-m)u_2 + \alpha]^2 < \Lambda_1$,
  (ii) $\det J_2 = (\Gamma_{11}\Gamma_{22} - \Gamma_{12}\Gamma_{21}) > 0$,   i.e., $\Lambda_2 > 0$,
  (iii) $(d_2\Gamma_{11} + d_1\Gamma_{22}) > 0$,   i.e., $\Lambda_3 > 0$,
  (iv) $d_2\Gamma_{11} + d_1\Gamma_{22} > 2\sqrt{d_1d_2(\det J_2)}$,   i.e., $\Lambda_3 > 2[(1-m)u_2 + \alpha]\sqrt{d_1d_2\Lambda_2}$,

where

$$
\begin{aligned}
\Lambda_3 &= 2d_1\gamma u_2 m\alpha - d_1\gamma u_2{}^2 m^2 - 2d_1\gamma u_2\alpha + d_2 u_2{}^2 + 2d_1\gamma u_2{}^2 m - 2d_2 u_2{}^3 + d_2\alpha^2 \\
&\quad + d_2\epsilon v_2 m\alpha - d_1\epsilon u_2 m\alpha + 4d_1\delta v_2 u_2{}^2 m - 4d_1\delta v_2 u_2\alpha - 2d_1\delta v_2 u_2{}^2 m^2 \\
&\quad + 4d_1\delta v_2 u_2 m\alpha - d_2\epsilon v_2\alpha + 4d_2 u_2{}^2 m\alpha - 2d_2 u_2 m\alpha + d_1\epsilon u_2\alpha - 2d_1\epsilon u_2{}^2 m \\
&\quad + d_1\epsilon u_2{}^2 m^2 - 2d_1\delta v_2\alpha^2 - 2d_1\delta v_2 u_2{}^2 - 2d_2 u_2{}^2 m - 4d_2 u_2{}^2\alpha + 4d_2 u_2{}^3 m \\
&\quad + d_2 u_2{}^2 m^2 + 2d_2 u_2\alpha - 2d_2 u_2\alpha^2 - 2d_2 u_2{}^3 m^2 + d_1\epsilon u_2{}^2 - d_1\gamma u_2{}^2 - d_1\gamma\alpha^2.
\end{aligned}
$$

In particular, we have $C(k^2) < 0 \Leftrightarrow k_1^2 < k^2 < k_2^2$, where k_1^2 and k_2^2 are the finite boundary wave number [30], can be obtained by the following form:

$$
k_{2,1}^2 = \frac{(d_1\Gamma_{22} + d_2\Gamma_{11}) \pm \sqrt{(d_1\Gamma_{22} + d_2\Gamma_{11})^2 - 4d_1d_2(\Gamma_{11}\Gamma_{22} - \Gamma_{12}\Gamma_{21})}}{2d_1d_2}.
$$

The results of Fig. 3 signifies that when d_2 is larger than the value marked by the red asterisk point in the figure, the Turing pattern emerges, other parameter values are $\alpha = 0.3$, $m = 0.2$, $\gamma = 0.02$, $\delta = 0.5$, $\epsilon = 1.0$, $d_1 = 0.1$. From Fig. 3 one can easily find that when $d_2 > 6.93$, there is a range of values for k for which $C(k^2) < 0$. This situation is clear from Fig. 4a and it can be noted that the range of $k \in (k_1, k_2)$ becomes wider with the increasing values of d_2. From Fig. 4b, it is clear that as d_2 increases, the available
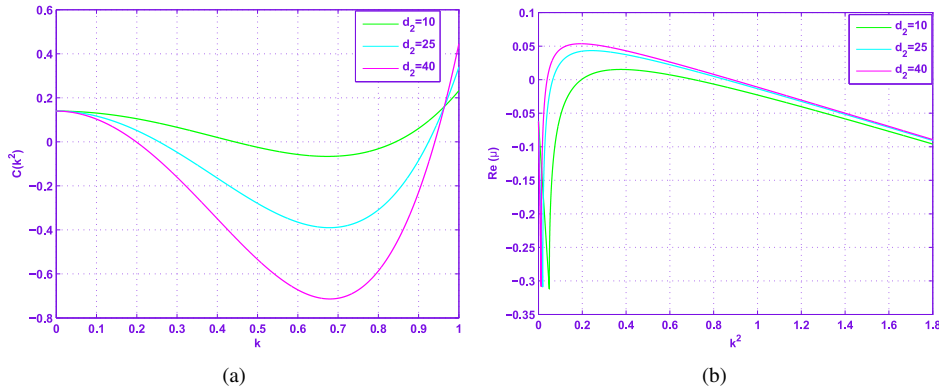
Fig. 4. Dispersion relation for different values of d_2 and other parameter values are $\alpha = 0.3$, $m = 0.2$, $\gamma = 0.02$, $\delta = 0.5$, $\epsilon = 1.0$, $d_1 = 0.1$.
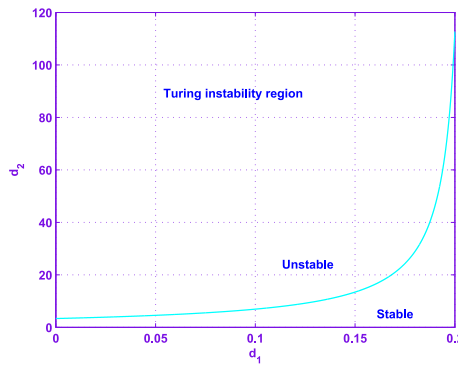

Fig. 5. Turing bifurcation diagram corresponding to $\alpha = 0.3$, $m = 0.2$, $\gamma = 0.02$, $\delta = 0.5$, $\epsilon = 1.0$ of model (4).

Turing modes $[\mathrm{Re}(\mu) > 0]$ also increase. The diffusive instability occurs when $d_2 > d_1$ which indicates that diffusivity of predator must be greater than that of the prey.

The Turing bifurcation breaks down the spatial symmetry, leading to the formation of patterns that are stationary in time and oscillatory in space [48] and occurs when $\mathrm{Im}(\mu(k)) = 0$, $\mathrm{Re}(\mu(k)) = 0$ at $k = k_T \neq 0$, where the wave number k_T satisfies $k_T^2 = \sqrt{\det J_2/(d_1 d_2)}$. Figure 5 shows the Turing instability region of system (4) in $d_1 d_2$-plane corresponding to $\alpha = 0.3$, $m = 0.2$, $\gamma = 0.02$, $\delta = 0.5$, $\epsilon = 1.0$.

The equilibria that can be found in Turing instability region, are stable with respect to homogeneous perturbations but unstable with respect to perturbations of specific wave number k and we have plotted contour pictures of Turing spatial pattern in this region.

5 Pattern formation

In earlier section, it has been shown that the non-trivial homogeneous stationary state can loose its stability when diffusion is taken into consideration. In this section, an extensive

numerical simulations of the spatially extended model (4) in two-dimensional space has been carried out and the behaviours of the qualitative results are exhibited through figures. The Turing pattern may be obtained by conducting appropriate numerical simulations because of the reason that the dynamic behaviour of the spatial model can not be investigated in detail by using analytical approaches usually due to various limitations. To solve a system of partial differential equations numerically, one has to discretize the space and time of the problem, i.e., transforming it from an infinite-dimensional (continuous) to a finite-dimensional (discrete) form. In practice, the continuous problem defined by the reaction–diffusion system in two-dimensional space is solved in a discrete domain with rectangular or square lattice sites. The present numerical simulations employ the nonzero initial condition with small random perturbation around homogeneous steady-state (u_2, v_2) and Neumann conditions at the domain boundary over a 200×200 lattice. In the present investigation, the diffusive terms in (4) is discretised using five point finite difference scheme and the forward Euler method has been used for time integration. For this purpose, the time stepsize has been selected to be $dt = 0.001$ and the space stepsize (lattice constant) to be $dx = dy = 0.5$ based upon the stability criterion for explicit scheme. In order to avoid numerical artifacts, it has been checked that a further decrease of the step sizes corresponding to both space and time did not lead to any significant modification of the results. The simulations were allowed to run until they reach a stationary state or until they show a behaviour that does not seem to change its characteristics anymore. In the simulations, different types of dynamics are observed and it has been found that the distributions of predator and prey are always of the same type.

The following Tables 1–2 symbolize the contour pictures of spatial pattern through diffusion-driven instability to the system (4) for different values of the diffusion coefficient d_2 and the refuge parameter m. The contour pictures of the time evolution of the interacting populations at different instants with or without prey refuge are nicely captured in Figs. 6–7 in order to describe various situations.

In all the cases, starting with a homogeneous steady state, the patterns take a long time to settle down, with the formation of spotted or stripe-like or coexistence of both patterns (cf. Figs. 6–7 and Tables 1–2). The results of the panels (a)–(d) of Fig. 6 exhibit the evolution of the spatial pattern of interacting populations in the absence of refuge (i.e., $m = 0$) at $t = 200$ and 500, with random perturbation of the steady state around $(u_2, v_2) = (0.071503106322443, 0.34493948021195)$ at $d_2 = 10$ and 40, respectively. At the stationary state, regular spots with the same radius prevail over the whole spatial domain and the dynamics of the system does not undergo any further changes which is

Table 1. The table shows the relevant values of parameters, time and contour pictures of Turing patterns.

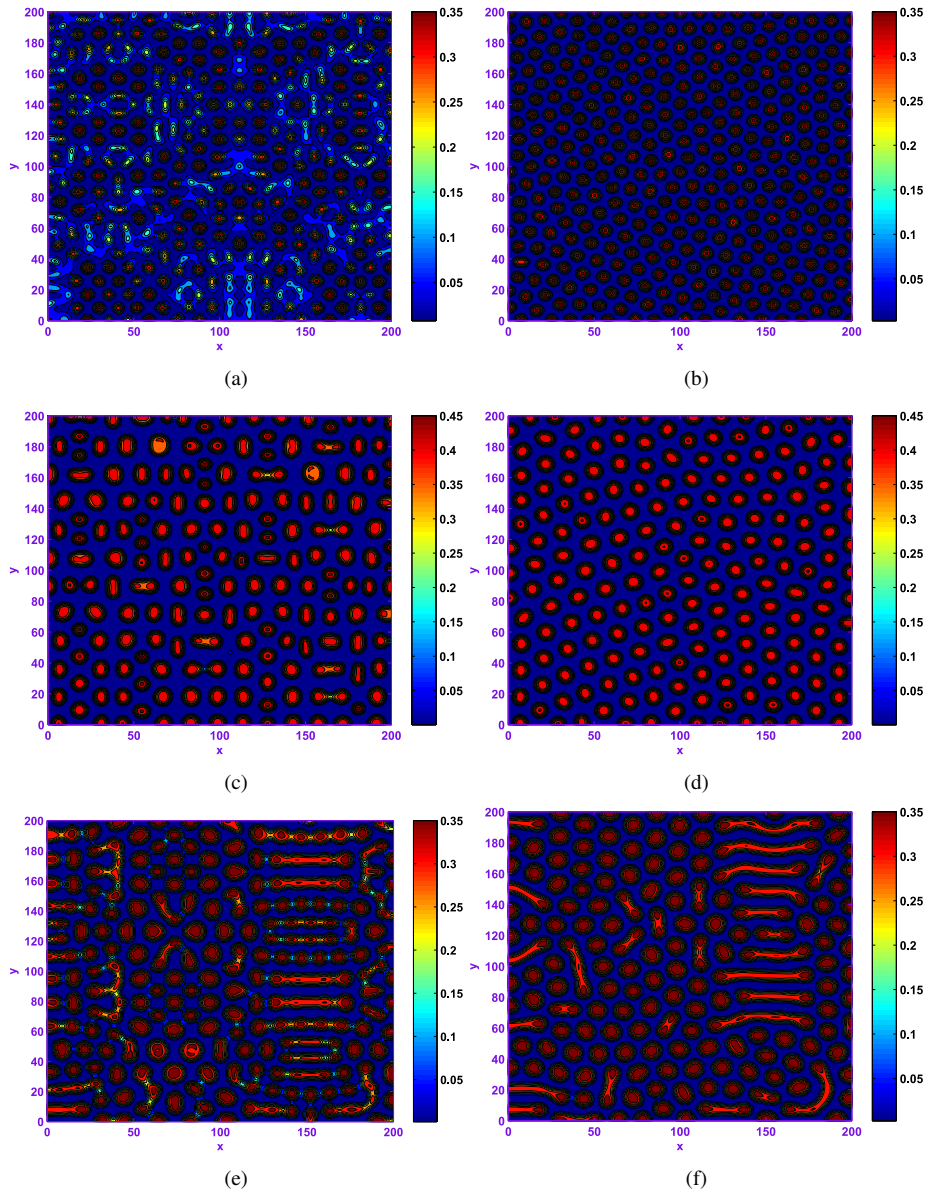| Values of diffusion and refuge parameters			Time	Contour pictures
$d_1 = 0.1,$	$d_2 = 10.0,$	$m = 0.0$	200	Fig. 6a
$d_1 = 0.1,$	$d_2 = 10.0,$	$m = 0.0$	500	Fig. 6b
$d_1 = 0.1,$	$d_2 = 40.0,$	$m = 0.0$	200	Fig. 6c
$d_1 = 0.1,$	$d_2 = 40.0,$	$m = 0.0$	500	Fig. 6d
$d_1 = 0.1,$	$d_2 = 40.0,$	$m = 0.2$	200	Fig. 6e
$d_1 = 0.1,$	$d_2 = 40.0,$	$m = 0.2$	500	Fig. 6f

(a)

(b)

(c)

(d)

(e)

(f)

Fig. 6. Snapshots of contour pictures of the time evolution of the prey species at different instants with $\alpha = 0.3$, $\gamma = 0.02$, $\delta = 0.5$, $\epsilon = 1.0$.

in good agreement with those of Wang et al. [48]. The significant feature is that (cf. panels (a), (b) and (c), (d) of Fig. 6) the lower and the upper bound for prey concentration over two-dimensional space is changing with the change of diffusion coefficients as well as the progression of time. Also it is evident that the difference between highest and

Table 2. The table shows the relevant values of parameters, time and contour pictures of Turing patterns.

Values of diffusion and refuge parameters			Time	Contour pictures
$d_1 = 0.1$,	$d_2 = 40.0$,	$m = 0.25$	200	Fig. 7a
$d_1 = 0.1$,	$d_2 = 40.0$,	$m = 0.25$	500	Fig. 7b
$d_1 = 0.1$,	$d_2 = 40.0$,	$m = 0.30$	200	Fig. 7c
$d_1 = 0.1$,	$d_2 = 40.0$,	$m = 0.30$	500	Fig. 7d

(a)   (b)

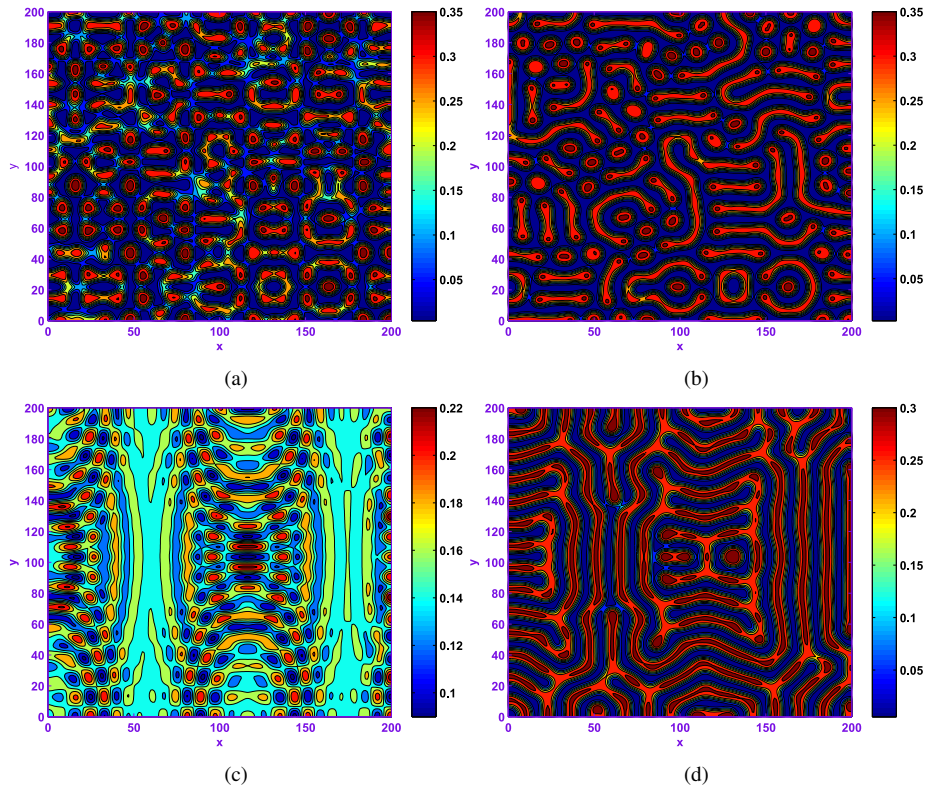(c)   (d)

Fig. 7. Snapshots of contour pictures of the time evolution of the prey species at different instants with $\alpha = 0.3$, $\gamma = 0.02$, $\delta = 0.5$, $\epsilon = 1.0$.

lowest concentration of prey species increases with the increase of d_2. Another interesting feature may be recorded by comparing the relevant figures (cf. panels (a), (b) and (c), (d) of Fig. 6 is that as d_2 increases, the radius of the spot increases irrespective of the number of iterations computed.

Three different types of spatial pattern can be obtained by varying the value of m (viz. 0.2 or 0.25 or 0.3), the refuge constant of the prey. One observes that both the spotted pattern and the stripe-like pattern coexist in the spatially extended model (4) corresponding to two different values of the refuge parameter $m = 0.2$ and $m = 0.25$ as shown in the panels (e), (f) of Fig. 6 and (a), (b) of Fig. 7, respectively. However, these

two patterns of panels (e) (f) of Fig. 6 and (a), (b) of Fig. 7 are essentially different from each other, because of their own different wavelengths. Likewise, the results of panels (c), (d) of Fig. 7 show the process of spatial pattern formation for the present model (4) with $m = 0.3$. In this case, the random perturbation around the homogeneous steady state $(u_2, v_2) = (0.1558461549, 0.4933383502)$ leads to the formation of spotted and stripe-like patterns, and ending with almost stripe-like patterns (cf. panels (c), (d) of Fig. 7), which is time independent. Examining all these spatial patterns one may notice that prey refuge plays a significant role in the formation of various kinds of patterns ranging from spot to stripe-like.

6   Conclusions and comments

The present investigation is primarily dealt with an in-depth analysis of the spatial pattern formation of a diffusive predator–prey system with intra-species competition among predators in the event of a prey refuge within two-dimensional space. The conditions of Turing space through diffusion-driven instability have been derived analytically. Analyzing the nature of the eigenvalues of the allied characteristic equations, the local and the global asymptotic stability analyses of the boundary equilibrium points e_0, e_1 along with the positive interior equilibrium point e_2 of the non-spatial model (4) have been reported at length. The system appears to attain Hopf-bifurcation at $\alpha = \alpha^{[HB]}$ (cf. Fig. 2 around e_2, where $\alpha^{[HB]}$ is given in Section 3.2 (iii).

The analytical derivation of the conditions in terms of the present system parameters for which the proposed diffusive predator–prey model with prey-dependent Holling type II functional response reveals the formation of spatial patterns through diffusion-driven instability. The influence of diffusion with prey refuge on the stability of the predator–prey coexistence equilibrium position has been focused with special attention in our proposed mathematical model. The distinguished feature is that the uniform steady state of a reaction–diffusion equation is stable for the ordinary differential equations, but it becomes unstable for the corresponding partial differential equations with diffusion resulting in the emergence of Turing instability. It is obvious from the results displayed through Figs. 6–7 that the number of the spotted (or stripe-like or coexistence of both) area in the spatial domain increases with increasing number of iterations for a particular set of parameter values. The mathematical analysis of the model system (4) shows that a reaction-diffusive predator–prey model regulates in a stable manner its growth around spatially homogeneous solutions via Turing instability mechanism. The results obtained from the model under consideration show that the influence of prey refuge plays an important role on the spatial pattern formation of the interacting populations.

More specifically, owing to the presence of prey refuge, the present dynamic model exhibits a change from spotted pattern to the stripe-like pattern as evident from Figs. 6–7. The spotted patterns do indicate that the prey populations are more isolated than the stripe-like patterns. Biologically one may interpret that when the ability of prey refuge is increased, the prey will be more centralized, i.e., the predator can not consume prey populations easily. One may also interpret this transition as, when the prey concentration

is high, prey have enough energy to prevent predator being caught or when the prey is in high density distribution, it is easy for them to capture the food for themselves. Thus, the results based on the present model show that the effect of the prey refuge for spatial pattern formation is profound on the dynamic complexity of ecosystems or physical systems.

7 Scope of future work

The influence of noise on nonlinear systems is the subject of intense experimental and theoretical investigations. The most well-known phenomenon is noise induces transition and stochastic resonance, both showing the possibility to transform noise in order. Recently, many eminent researchers through their investigations have revealed that noise can have an important impact on the dynamics of ecological populations [2, 43, 50]. The comprehension of noise's role in the dynamics of nonlinear systems plays a key aspect in the efforts devoted to understand and then to model so-called complex ecosystems. A large volume of work has already been carried out by taking into account the influence of noise in ecologically relevant models of ordinary differential equations or partial differential equations with logistic growth. Sun et al. [44] showed that when the diffusive predator–prey model has no noise, it exhibits wave dynamics in two-dimensional space, however, combined with noise, it exhibits chaotic patterns. Li and Zhen [24] illustrated pattern dynamics of a spatial predator–prey model with noise and they concluded that when the noise intensity and temporal correlation are in appropriate levels, the model exhibis phase transition from spotted to stripe pattern. However, it has been observed in the literature that the refuge effect by the prey species, especially combined with diffusion of the spatial patterns, had been generally overlooked, despite its potential ecological reality and intrinsic theoretical interest. These structures may in fact correspond to the real world. For this reason, one may investigate the effect of noise on the spatial patterns of a predator–prey model with the effect of prey refuge. The environments in models and also laboratories are much less complex than ecological environments. The deterministic environment is rarely the case in real life. Natural environments are random environments, therefore the inclusion of noise sources in the proposed mathematical model (4) could give more realistic results from physical point of view. This is desirable in future studies.

Appendix

Let us consider a function $H(u, v)$ of the form $H(u, v) = 1/(uv)$. Then $H(u, v) > 0$ for both $u, v > 0$. Now

$$G(u, v) = \frac{\partial}{\partial u}(F_1 H) + \frac{\partial}{\partial v}(F_2 H),$$

where F_1 and F_2 are the right hand side of the non-spatial system of (4). By Bendixon–Dulac criterion, one can see that if $\epsilon \leqslant 2\epsilon\delta/(1 - m)$, then $G(u, v) < 0$; therefore,

the system has no non-trivial positive periodic solution. Also, $\limsup_{t \to +\infty} u(t) \leqslant \overline{u}$, $\limsup_{t \to +\infty} v(t) \leqslant \overline{v}$, $\liminf_{t \to +\infty} u(t) \geqslant \underline{u}$ and $\liminf_{t \to +\infty} v(t) \geqslant \underline{v}$, where $\overline{u} = 1$, $\overline{v} = (\epsilon - \gamma)/\delta$, $\underline{u} = (1 \pm \sqrt{1 - 4\epsilon \underline{v}})/2$ and $\underline{v} = ((\epsilon - \gamma)(1 - m)\underline{u} - \alpha\gamma)/\delta((1 - m)\underline{u} + \alpha)$. Therefore, the conditions for global stability are $\gamma < \epsilon \leqslant 2\epsilon\delta/(1 - m)$ and $\underline{v} > 0$, see [13, 14] for details. These together with the assumption of local stability yield the conclusion.

References

1. P.A. Abrams, L.R. Ginzburg, The nature of predation: Prey dependent, ratio dependent or neither?, *Trends Ecol. Evol.*, **15**(8):337–341, 2000.

2. P. Aguirre, E. González-Olivares, S. Torres, Stochastic predator–prey model with allee effect on prey, *Nonlinear Anal., Real World Appl.*, **14**(1):768–779, 2013.

3. S. Aly, I. Kim, D. Sheen, Turing instability for a ratio-dependent predator–prey model with diffusion, *Appl. Math. Comput.*, **217**:7265–7281, 2011.

4. A.D. Bazykin,*Nonlinear Dynamics of Interacting Populations*, Nonlinear Science Series A, Vol. 11, World Scientific, Singapore, 1998.

5. F. Chen, L. Chen, X. Xie, On a leslie-gower predator–prey model incorporating a prey refuge, *Nonlinear Anal., Real World Appl.*, **10**(5):2905–2908, 2009.

6. S. Chen, J. Shi, Global stability in a diffusive Holling–Tanner predator–prey model, *Appl. Math. Lett.*, **25**(3):614–618, 2012.

7. J.H. Connell, A predator–prey system in the marine intertidal region. I. *Balanus glandula* and several predatory species of Thais, *Ecol. Monogr.*, **40**(1):49–78, 1970.

8. A. Gierer, H. Meinhardt, A theory of biological pattern formation, *Kybernetik*, **12**(1):30–39, 1972.

9. E. González-Olivares, R. Ramos-Jiliberto, Dynamic consequences of prey refuges in a simple model system: More prey, fewer predators and enhanced stability, *Ecol. Model.*, **166**(1):135–146, 2003.

10. E. González-Olivares, R. Ramos-Jiliberto, Consequences of prey refuge use on the dynamics of some simple predator–prey models: Enhancing stability?, in R. Mondaini (Ed.) *Proceedings of the Third Brazilian Symposium on Mathematical and Computational Biology, Vol. 2*, E-Papers Serviços Editoriais, Rio de Janeiro, 2004, pp. 75–98.

11. X. Guan, W. Wang, Y. Cai, Spatiotemporal dynamics of a Leslie–Gower predator–prey model incorporating a prey refuge, *Nonlinear Anal., Real World Appl.*, **12**(4):2385–2395, 2011.

12. G.-Q. Sun, Z. Jin, Q.-X. Liu, L. Li, Pattern formation induced by cross-diffusion in a predator–prey system, *Chin. Phys. B*, **17**(11):3936–3941, 2008.

13. M. Haque, Ratio-dependent predator–prey models of interacting populations, *Bull. Math. Biol.*, **71**(2):430–452, 2009.

14. M. Haque, A detailed study of the Beddington–DeAngelis predator–prey model, *Math. Biosci.*, **234**(1):1–16, 2011.

15. M. Haque, Existence of complex patterns in the Beddington–DeAngelis predator–prey model, *Math. Biosci.*, **239**(2):179–190, 2012.

16. M.P. Hassell, *The Dynamics of Arthropod Predator–Prey Systems*, Princeton Univ. Press, Princeton, NJ, 1978.

17. Y. Huang, F. Chen, L. Zhong, Stability analysis of a prey–predator model with Holling type III response function incorporating a prey refuge, *Appl. Math. Comput.*, **182**(1):672–683, 2006.

18. L. Ji, C. Wu, Qualitative analysis of a predator–prey model with constant-rate prey harvesting incorporating a constant prey refuge, *Nonlinear Anal., Real World Appl.*, **11**(4):2285–2295, 2010.

19. D.W. Jordan, P. Smith, *Nonlinear Ordinary Differential Equations: An introduction to Dynamical Systems, Vol. 2*, Oxford Univ. Press, 1999.

20. H. Katsuragi, Diffusion-induced spontaneous pattern formation on gelation surfaces, *Europhys. Lett.*, **73**:793–799, 2006.

21. W. Ko, K. Ryu, Qualitative analysis of a predator–prey model with Holling type II functional response incorporating a prey refuge, *J. Differ. Equations*, **231**(2):534–550, 2006.

22. V. Krivan, Effects of optimal antipredator behavior of prey on predator–prey dynamics: The role of refuges, *Theor. Popul. Biol.*, **53**(2):131–142, 1998.

23. S.A. Levin, L.A. Segel, Hypothesis for origin of planktonic patchiness, *Nature*, **259**, 659, 1976.

24. L. Li, Z. Jin, Pattern dynamics of a spatial predator–prey model with noise, *Nonlinear Dyn.*, **67**(3):1737–1744, 2012.

25. Z. Li, M. Gao, C. Hui, X. Han, H. Shi, Impact of predator pursuit and prey evasion on synchrony and spatial patterns in metapopulation, *Ecol. Model.*, **185**(2–4):245–254, 2005.

26. S. Magalhaes, P.C.J Van Rijn, M. Montserrat, A. Pallini, M.W. Sabelis, Population dynamics of thrips prey and their mite predators in a refuge, *Oecologia*, **150**(4):557–568, 2007.

27. R.M. May, *Stability and Complexity in Model Ecosystems, Vol. 6*, Princeton Univ. Press, Princeton, NJ, 2001.

28. J.N. McNair, The effects of refuges on predator–prey interactions: A reconsideration, *Theor. Popul. Biol.*, **29**(1):38–63, 1986.

29. J.J. Meyer, J.E. Byers, As good as dead? Sublethal predation facilitates lethal predation on an intertidal clam, *Ecol. Lett.*, **8**(2):160–166, 2005.

30. J.D. Murray, *Mathematical Biology*, Springer-Verlag, Berlin, 1993.

31. A. Okubo, *Diffusion and Ecological Problems: Mathematical Models*, Springer-Verlag, Berlin, 1980.

32. A. Okubo, S.A. Levin, *Diffusion and Ecological Problems: Modern Perspectives*, Springer-Verlag, Berlin, 2001.

33. A. Pallini, A. Janssen, M.W. Sabelis, Predators induce interspecific herbivore competition for food in refuge space, *Ecol. Lett.*, **1**:171–176, 1998.

34. R. Peng, M. Wang, G. Yang, Stationary patterns of the Holling–Tanner prey–predator model with diffusion and cross-diffusion, *Appl. Math. Comput.*, **196**(2):570–577, 2008.

35. G.D. Ruxton, Short term refuge use and stability of predator–prey models, *Theor. Popul. Biol.*, **47**(1):1–17, 1995.

36. S. Sarwardi, P.K. Mandal, S. Ray, Analysis of a competitive prey–predator system with a prey refuge, *Biosystems*, **110**(3):133–148, 2012.

37. L.A. Segel, J.L. Jackson, Dissipative structure: An explanation and an ecological example, *J. Theor. Biol.*, **37**(3):545–559, 1972.

38. A. Sih, Prey refuges and predator–prey stability, *Theor. Popul. Biol.*, **31**(1):1–12, 1987.

39. G.-Q. Sun, S. Sarwardi, P.J. Pal, S. Rahaman, The spatial patterns through diffusion-driven instability in modified Leslie–Gower and Holling-type II predator–prey model, *J. Biol. Syst.*, **18**(3):593–603, 2010.

40. G.-Q. Sun, G. Zhang, Z. Jin, L. Li, Predator cannibalism can give rise to regular spatial pattern in a predator–prey system, *Nonlinear Dyn.*, **58**(1):75–84, 2009.

41. G.-Q. Sun, Z. Jin, L. Li, M. Haque, B.-L. Li, Spatial patterns of a predator–prey model with cross diffusion, *Nonlinear Dyn.*, **69**(4):1631–1638, 2012.

42. G.-Q. Sun, Z. Jin, L. Li, B.-L. Li, Self-organized wave pattern in a predator–prey model, *Nonlinear Dyn.*, **60**(3):265–275, 2010.

43. G.-Q. Sun, Z. Jin, L. Li, Q.-X. Liu, The role of noise in a predator–prey model with allee effect, *J. Biol. Phys.*, **35**(2):185–196, 2009.

44. G.-Q. Sun, Z. Jin, Q.-X. Liu, B.-L. Li, Rich dynamics in a predator–prey model with both noise and periodic force, *Biosystems*, **100**(1):14–22, 2010.

45. G.-Q. Sun, Z. Jin, Q.-X. Liu, L. Li, Dynamical complexity of a spatial predator–prey model with migration, *Ecol. Model.*, **219**(1):248–255, 2008.

46. R.J. Taylor, *Predation*, Chapman & Hall, New York, 1984.

47. A.M. Turing, The chemical basis of morphogenesis, *Philos. Trans. R. Soc. London, Ser. B*, **237**(641):37–72, 1952.

48. W. Wang, Q.-X. Liu, Z. Jin, Spatiotemporal complexity of a ratio-dependent predator–prey system, *Phys. Rev. E*, **75**(5), 051913, 9 pp., 2007.

49. Y. Wang, J. Wang, Influence of prey refuge on predator–prey dynamics, *Nonlinear Dyn.*, **67**(1):191–201, 2011.

50. X.-C. Zhang, G.-Q. Sun, Z. Jin, Spatial dynamics in a predator–prey model with Beddington–DeAngelis functional response, *Phys. Rev. E*, **85**(2), 021924, 14 pp., 2012.